HHS Public Access

Author manuscript

Am J Med Genet C Semin Med Genet. Author manuscript; available in PMC 2021 September 01.

Published in final edited form as:

Am J Med Genet C Semin Med Genet. 2020 September ; 184(3): 618–630. doi:10.1002/ajmg.c.31823.

The peroxisomal disorder spectrum and Heimler syndrome: Deep phenotyping and review of the literature

Malena Daich Varela[1], **Priyam Jani**[2], **Wadih M. Zein**[1], **Precilla D'Souza**[3], **Lynne Wolfe**[4], **Jennifer Chisholm**[5], **Christopher Zalewski**[5], **David Adams**[3,4], **Blake M. Warner**[2], **Laryssa A. Huryn**[1], **Robert B. Hufnagel**[1]

[1]Ophthalmic Genetics and Visual Function Branch, National Eye Institute, National Institutes of Health (NIH), Bethesda, Maryland [2]National Institute of Dental and Craniofacial Research, NIH, Bethesda, Maryland [3]Office of the Clinical Director, National Human Genome Research Institute, NIH, Bethesda, Maryland [4]Undiagnosed Diseases Program, Common Fund, NIH, Bethesda, Maryland [5]Audiology Unit, Otolaryngology Branch, National Institute on Deafness and Other Communication Disorders, NIH, Bethesda, Maryland

Abstract

The spectrum of peroxisomal disorders is wide and comprises individuals that die in the first year of life, as well as people with sensorineural hearing loss, retinal dystrophy and amelogenesis imperfecta. In this article, we describe three patients; two diagnosed with Heimler syndrome and a third one with a mild-intermediate phenotype. We arrived at these diagnoses by conducting complete ophthalmic (National Eye Institute), auditory (National Institute of Deafness and Other Communication Disorders), and dental (National Institute of Dental and Craniofacial Research) evaluations, as well as laboratory and genetic testing. Retinal degeneration with macular cystic changes, amelogenesis imperfecta, and sensorineural hearing loss were features shared by the three patients. Patients A and C had pathogenic variants in *PEX1* and Patient B, in *PEX6*. Besides analyzing these cases, we review the literature regarding mild peroxisomal disorders, their pathophysiology, genetics, differential diagnosis, diagnostic methods, and management. We suggest that peroxisomal disorders are considered in every child with sensorineural hearing loss and retinal degeneration. These patients should have a dental evaluation to rule out amelogenesis imperfecta as well as audiologic examination and laboratory testing including peroxisomal biomarkers and genetic testing. Appropriate diagnosis can lead to better genetic counseling and management of the associated comorbidities.

Keywords

amelogenesis imperfect; heimler syndrome; peroxisomal disorders; retinal degeneration; sensorineural hearing loss

Correspondence Robert B. Hufnagel, Ophthalmic Genetics and Visual Function Branch, National Eye Institute, National Institutes of Health, 10 Center Drive, Building 10, 10N109, Bethesda, MD 20892. robert.hufnagel@nih.gov.
Laryssa A. Huryn and Robert B. Hufnagel are co-senior authors.

1 | INTRODUCTION

Peroxisomal disorders are represented by a wide spectrum of clinical manifestations ranging from death in the first year of life to sensorineural hearing loss, retinal dystrophy, and amelogenesis imperfecta (Klouwer et al., 2015). They can be classified into two groups taking into account their pathophysiology: peroxisomal biogenesis disorders (PBDs) and peroxisomal enzyme deficiencies (PEDs). The former are caused by a failure in the development of the organelle, including its membranes, matrix, and assembly. PEDs on the other hand, are due to the absence or misfunction of one or more metabolic reactions that take place within the peroxisome (Tan, Gonçalves, Almehdar, & Soares, 2018). PBDs are secondary to variants in the *PEX* genes family whereas PEDs are a genetically heterogeneous group, involving variants in *ABCD1*, *ACOX1*, and *PAHX*, among others (Tan et al., 2018).

The majority of individuals with PBDs (80%) are diagnosed with Zellweger spectrum disorders (ZSDs) while 20% have peroxisomal fission defects and rhizomelic chondrodysplasia punctate (S. Steinberg et al., 2004). ZSDs have an estimated prevalence of 1:50,000 births (Delille, Bonekamp, & Schrader, 2006; Vasiljevic et al., 2019). This group of disorders includes Zellweger syndrome (ZS), neonatal adrenoleukodystrophy (NALD), infantile Refsum disease (IRD), and Heimler syndrome (HS) (Klouwer et al., 2015). ZS is the most common and severe form of ZSDs and is also known as cerebro-hepato-renal syndrome (Lee & Raymond, 2013). It was first described in 1969 and the link with peroxisomes was discovered in 1973, after a hepatic and renal biopsy of two young patients showed absence of these organelles (Goldfischer et al., 1973; Opitz, 1969). A few years later, an increased concentration of very long chain fatty acids (VLCFA) was measured in the plasma of patients with this condition, providing a biomarker for diagnosis (Brown 3rd et al., 1982). In 1984, IRD and NALD patients were found to have similar biochemical abnormalities to ZS patients (Kelley & Moser, 1984; Poulos, Sharp, & Whiting, 1984), which led to the discovery of peroxisomes as their pathophysiologic mechanism, thus grouping them as ZSDs. HS was added to this group in 2015. First characterized in 1991, its molecular etiology had remained unknown (Heimler, Fox, Hershey, & Crespi, 1991; Lima et al., 2011; Ratbi et al., 2015) due to its milder phenotype when compared with the rest of the PBDs, and the lack of neurologic manifestations (Ventura et al., 2016).

1.1 | Heimler syndrome's clinical features

In the initial report, HS was described as a triad of sensorineural hearing loss, enamel hypoplasia and nail abnormalities (Heimler et al., 1991). Severe to profound hearing loss can be unilateral or bilateral and usually appears in the first decade of life (Ong, Visram, McKaig, & Brueton, 2006). Enamel hypoplasia is noted as yellow-brown teeth with a granular appearance. Secondary teeth are mostly affected, more severely molars and premolars (the posterior teeth), with spared permanent incisors. Primary dentition is usually normal (Ong et al., 2006). Nails abnormalities are characterized by ridging (Beau's lines) and punctate leukonychia, present on both toe and fingernails. These signs have been associated with a number of conditions (e.g., anemia, zinc deficiency, as an adverse effect of chemotherapy, microtrauma, Raynaud's syndrome) (Bodman, 2004). In a recent review, they

were found in up to 40% of the patients with HS, therefore they do not appear to be a sensitive, specific component of the phenotyope (Gao et al., 2019). Lima et al. found that patients with HS may also have retinal and macular dystrophies, causing decreased visual acuity (Lima et al., 2011). No dysmorphism, neurological features, or intellectual disability was found in these patients (Ratbi et al., 2015).

1.2 | Diagnosis

Many patients fail newborn hearing screening, thus becoming the first diagnostic clue of the condition (N. Braverman, Argyriou, & Moser, 2014). Biochemical tests are usually within normal limits in patients with HS (Ratbi et al., 2015; Zeharia et al., 2007). However, since plasma abnormalities may be an important clue to diagnose a severe peroxisomal disease, a routine peroxisomal panel for these patients is recommended. This should include the measurement of the plasma concentration of large molecules such as VLCFA (fatty acids of 22 carbons or longer), molecules degraded by peroxisomes in a normal setting. Particularly, an elevated concentration as well as increased ratios of C24:0/C22:0 and C26:0/C22:0 are highly specific for peroxisomal disorders (N. E. Braverman et al., 2016). False positives are reported in the literature in nonfasting conditions or ketogenic diets, and normalization of VLCFA with age has also been reported (Lipiński et al., 2020; Theda, Woody, Naidu, Moser, & Moser, 1993). Elevated levels of C26:0-lysophosphatidylcholine (C26:0-lysoPC) have been associated with a sensitivity of 89.2% in patients with a ZSD, being a useful marker for VLCFA accumulation (Klouwer et al., 2017). Also, specific to ZSDs, phytanic and pristanic acids are found elevated in plasma and/or urine. In newborns, the diagnostic yield is better in urine and as the child grows, a blood sample becomes the recommended option (Peduto et al., 2004). False negatives may occur if the infant is not consuming dairy, ruminant animal fats, or fish (S. Steinberg, Jones, Tiffany, & Moser, 2008). Reduced levels of erythrocyte plasmalogens can also be measured in blood, and elevated bile acids intermediates are present both in plasma and urine (Wanders & Waterham, 2006).

As an alternative if available, a more sensitive way of testing the function of the peroxisomes is by culturing patient fibroblasts and measuring the peroxisomal activity within those cells (S. Steinberg et al., 2008). This can be done by quantifying the VLCFA oxidation or the concentrations of these macromolecules, phytanic, and pristanic acid intracellularly. Newborn screening rules out high concentrations of VLCFA which, as mentioned before, may or may not be elevated in the mildest phenotypes. Prenatal diagnosis uses either biochemical or genetic testing, the latter being more sensitive (N. E. Braverman et al., 2016).

1.3 | Genetics

Genetic testing is the most sensitive diagnostic method for HS, and oftentimes the only positive laboratory finding (79% of the patients reported to date have a molecular diagnosis) (Gao et al., 2019; Ratbi et al., 2015). Particularly, variants in *PEX1*, *PEX6*, and *PEX26* have been associated with HS (Neuhaus et al., 2017; Ratbi et al., 2015). These genes have been also related with other more severe conditions within the ZSD spectrum. *PEX1* is the mutated gene in around 60% of the patients with PBDs, while *PEX6* is involved in around 10% of the cases (Mechaussier, Marlin, Kaplan, Rozet, & Perrault, 2019; S. Steinberg et al., 2004; S. J. Steinberg, Raymond, Braverman, & Moser, 2017). Several authors have sought to

address whether genotype–phenotype correlations exist by functional testing. Rosewich et al. and Walter et al. reported a severer phenotype in patients with nearly abolished PEX1 protein levels when compared to patients with residual levels. The latter was found in patients with missense variants while the more severe was due to insertions, deletions, and splicing variants (Rosewich, 2005; Walter et al., 2001). Similar genotype–phenotype correlation was established for *PEX6*; nonsense and frame-shift more often causing severe disease whereas missense with residual protein activity being associated with a milder phenotype (Smith et al., 2016).

In this seminar, we present three unrelated patients with mild, late-onset peroxisomal disease that underwent comprehensive ophthalmic and dental evaluation. We also review the basis of PBDs and highlight the spectrum of tissue-level disease and age-of-onset in relationship to variants in the *PEX* gene family.

2 | METHODS

All patients were evaluated at the National Eye Institute (NEI) and National Institute of Dental and Craniofacial Research (NIDCR) within the National Institutes of Health (NIH, Bethesda, MD). Patients A and B were also examined at the National Institute of Deafness and Other Communication Disorders (NIDCD). The patients were consented to NEI sponsored, Institutional Review Board approved, clinical research protocols for screening and evaluation of potential research participants and study the genetics of inherited eye diseases (NCT02471287). Patient C was also consented to a protocol for clinical and genetic evaluation of patients with undiagnosed disorders through the Undiagnosed Diseases Network (NCT02450851), from the National Human Genome Research Institute (NHGRI). The study protocols adhered to the tenets of the Declaration of Helsinki and complied with the Health Insurance Portability and Accountability Act.

2.1 | Ophthalmic evaluation

A thorough ophthalmic evaluation was performed, including measurement of best corrected visual acuity, motility and alignment exam, slit lamp and dilated fundus evaluation. Additional testing included color vision testing by Farnsworth D15 panel and Ishihara color plates test, optical coherence tomography (OCT) (Carl Zeiss Meditec AG, Dublin, CA), color and autofluorescence retinal imaging (Optos ultrawide-field retinal imaging device, Dunfermline, Scotland), Goldmann kinetic perimetry (Goldmann perimeter, Haag-Streit AG). International Society for Clinical Electrophysiology of Vision (ISCEV) standard full-field electroretinograms (ERG) were recorded using a commercial electrophysiology system (LKC, Gaithersburg, MD) (Marmor et al., 2008; McCulloch et al., 2014).

2.2 | Dental evaluation

The oral and dental evaluation included a detailed clinical exam consisting of the inspection of the oral structures and soft tissue, including the palate, uvula, and gingiva. The dental and hard tissue evaluation included the occlusion, eruption pattern, tooth morphology, jaw relationship, and TMJ function. Cone-beam computed tomography (Planmeca Promax 3D Max, Planmeca USA Inc., IL; 200 μm resolution) and intraoral photography (Canon EOS

5D Mark II camera, Canon USA Inc., VA) were performed to further assess dental phenotypes including findings such as tooth impaction, dental decay, and enamel defects. For each patient, seven intraoral photos were taken: the frontal view of dentition in occlusion, the frontal view of dentition at rest (2–3 mm leeway space), the maxillary arch, the mandibular arch, the left lateral view (maxillary and mandibular teeth in occlusion), the right lateral view, and the oropharyngeal region. three-dimensional (3D) intra oral scans were performed using the 3shape Trios 3 Color (3shape A/S, Denmark) intraoral scanner.

The severity of enamel defects was graded using a classification system for enamel defects reported previously (Jani et al., 2020). The classification of dental enamel defects was applied for both deciduous and permanent dentitions. Briefly, the enamel loss was measure by the amount of tooth surface affected and the number of teeth affected.

Cone-beam computed tomography (CBCT) images were used to generate panoramic X-rays and individual tooth slices using Planmeca Romexis software. CBCT images were exported to AnalyzePro software (Analyze Direct) for volume and thickness analyses. Images were cropped to mandibular first molar region. Enamel and dentin in mandibular first molars from each patient were segmented to calculate the volumes in the crown portion of the tooth. Bone microarchitecture addon in Analyzepro was used to assess the enamel thickness.

2.3 | Audiometric evaluation

Patients A and B were evaluated at the NIH for comprehensive audiologic examinations, which were conducted using GSI-AudioStar Pro (Grason-Stadler, Eden Prairie, MN) clinical audiometers with the patient seated in a double-walled sound treated rooms, both of which met American National Standards Institute criteria. Speech and pure-tone thresholds from 250 to 8,000 Hz were obtained from each ear using insert earphones via conventional audiometric procedures. Middle ear measures were acquired using a Grason Stadler GSI-Tympstar immittance bridge. Distortion Product Otoacoustic Emissions (DPOAEs) (ILO296 Otodynamics, Inc.) were measured in quarter octave bands over the frequency range of 842–7,996 Hz. Patient C presented to the NIH with bilateral cochlear implantation and subsequent behavioral hearing assessment was deferred. Outside audiometric records were available for review.

2.4 | Diagnosis

Each patient provided blood, from which genomic DNA was extracted and Next Generation Sequencing (NGS)-based genetic diagnostic tests were performed. Patients A and B were tested for variants in a Retinal Dystrophy panel, consisting of 325 genes (Blueprint Genetics, CLIA: 99D2092375). Patient C underwent Exome Sequencing. Pathogenic and likely pathogenic variants were further confirmed by bidirectional Sanger sequencing. Copy Number Variations (deletions/duplications) were screened in Patients A and B using a quantitative-PCR assay. After Sanger validation and segregation analysis, ACMG guidelines (Richards et al., 2015) were used to classify the variants for pathogenicity.

A peroxisomal panel was also analyzed in the blood sample of all patients, including the measurements of: C22:0, C24:0, C26:0, C24:0/C22:0, Q26.0/Q22.0, pristanic acid, phytanic acid, and pristanic/phytanic acid.

3 | RESULTS

3.1 | Clinical evaluation

Patient A was a 30-year-old woman who came to the Ophthalmic Genetics clinic for an evaluation of her cystic macular changes. At approximately 17 years of age she underwent her first ophthalmic exam due to decreased central vision and night blindness (nyctalopia), where she was diagnosed with cystic macular degeneration. She did not report issues with color or side vision at that time. Her medical history was positive for high frequency hearing loss beginning at 4 years of age and she had been wearing hearing aids since age of five. She had an autosomal dominant family history of juvenile onset high frequency hearing loss without other pertinent family history and reported long-standing tinnitus and a childhood history significant for multiple sets of pressure equalization tubes due to chronic middle ear disease. The patient did not report issues with primary teeth, but her molars started showing signs of amelogenesis imperfecta during childhood. She had one episode of uncomplicated kidney stone and her surgical history was positive for cholecystectomy.

Her best corrected visual acuity (BCVA) was 20/125 in her right eye (OD) and 20/25 in her left eye (OS), using a mild hyperopic correction. Her intraocular pressure (IOP) was within normal limits (16 mmHg OD and OS). Her axial length was shorter than the average (Oliveira et al., 2007) (20.30 OD and 20.34 OS), and she had steep corneas (K1 48.98, K2 47.80). Her color discrimination showed a deficit in the right eye (10 errors in Farnsworth D15) but was normal in the left eye. By Goldmann kinetic perimetry, both eyes were remarkably symmetrical, showing preserved peripheral vision with the V4e isopter. Testing the I4e isopter (smaller stimulus), a temporal scotoma was noticed paracentrally. A functional central scotoma was also detected by testing smaller and dimmer stimuli, I2e and I1e. Her ERG showed decreased amplitude for both dark and light adapted responses, with delayed timing only in the cone flicker. Her macular OCT showed cystic spaces in a 3 mm circumference around the center of fixation, retinal thinning (central macular thickness [CMT] was 123 μm OD and 198 μm OS) and loss of the retinal outer layers in both eyes, with a foveolar sparing on the left eye (Figure 1a). Her fundus exam showed retinal vascular attenuation, mottled appearance of the retinal pigment epithelium (RPE), minimal pigment migration and optic disc pallor. Autofluorescence imaging revealed a hypo-hyperautofluorescence pattern affecting the posterior pole and midperiphery (Figure 1b).

She had an adult dentition with 28 permanent teeth. She had mild loss of enamel on occlusal surface of upper (maxillary) and lower (mandibular) molars (Figure 2a). The enamel loss was graded as Grade 2 (Figure 2d) as it involved only one surface out of five and affected 8 teeth out of 28. The enamel loss on the molars led to attrition and flattening of the occlusal surfaces. The patient had root canal treatment with one tooth (#7) and prosthetic crown with tooth #31 as seen in panoramic X-ray (Figure 3a). Several restorations were placed on occlusal surface due to enamel loss. The CBCT scans showed normal enamel on the anterior teeth, but thinner layer of enamel on molars teeth (red arrow heads, Figure 3d). Audiometric evaluation documented a bilateral, symmetrical, mild to severe sensorineural hearing loss with mildly reduced speech discrimination ability at elevated listening levels (Figure 4). Middle ear function testing revealed normal middle ear pressure and mobility bilaterally

with an appropriate absence of acoustic stapedial reflexes and DPOAEs in each ear providing evidence to support a cochlear contribution to the hearing loss in each ear. Her fingernails were bowed and wavy past the fingertip and no leukonychia or abnormal coloration was noted. Abdominal ultrasound revealed normal liver and kidneys.

Patient B was a 17-year-old female who was referred for evaluation due to possible retinal degeneration. She had recently noticed decreased vision in her right eye when incidentally occluding her left eye and had no other reported difficulties with dim light, color and side vision.

She reports a diagnosis of bilateral sensorineural hearing loss at age 4 years with a history of binaural hearing aid use since that time. History is negative for middle ear disease with the exception of a single reported ear infection in her early teenage years. Her secondary teeth had enamel issues, while the primary dentition was reportedly normal. She had shorter stature than her parents and possible skeletal issues noticed after a radial fracture, where her bone “grew back together” after two surgeries. She did not have balance, liver or kidney problems. As a family history, her maternal grandmother had Bardet-Biedl syndrome, presenting with severe retinal degeneration, postaxial polydactyly and hepatic and renal failure.

Our evaluation revealed a BCVA of 20/160 OD and 20/20 OS, using a mild hyperopic correction. IOP, keratometry and axial length were unremarkable. She had 12 errors in the D15 color discrimination test with the right eye, and no errors in the left eye. Her visual field testing was only positive for central functional scotomas on both eyes, showing preserved periphery. An electroretinogram demonstrated only mildly delayed cone flicker, with normal amplitudes in photopic and scotopic tests. Her CMT was significantly increased in her right eye (927 μm), showing large cystic spaces disrupting the macular layers. Her left eye's macular thickness was 275 μm, and it also presented cysts of smaller diameter (Figure 1c). Her fundus exam showed a mottled appearance in the posterior pole and mid periphery, along with mild retinal vascular attenuation. This area appeared mostly hyperautofluorescent in imaging, with a few spots of hypoautofluorescence (Figure 1d). She had adult dentition with severe loss of enamel with 20 of 28 permanent teeth affected and all tooth surfaces having enamel loss (Grade 4, Figure 2b). Her upper and lower anterior teeth (incisors) had most enamel retained. The enamel loss resulted in altered tooth morphology of the posterior teeth (Figure 2d) and reduced height of the occlusal plane. Both maxillary first molars (# 3,14) had broken crowns due to weak enamel leading to exposed pulp cavity although the patient was asymptomatic (asterisk, Figure 2b). Panoramic X-rays show restorations on two teeth (#7,10) and crown on tooth #19 (Figure 3b). CBCT showed irregular and thin enamel on anterior teeth (red arrow heads, Figure 3e) whereas posterior teeth had no enamel on occlusal surface and thin enamel on proximal surfaces. Audiometric evaluation revealed a bilateral moderate to profound sensorineural hearing loss bilaterally with a severe reduction in speech discrimination ability at significantly elevated listening levels in each ear (Figure 4). Middle ear function testing revealed normal middle ear pressure and mobility bilaterally with an appropriate absence of acoustic stapedial reflexes and DPOAEs in each ear providing evidence to support a cochlear contribution to the hearing loss in each ear. Her fingernails were mostly normal, with only one spot of leukonychia on a fingernail.

Patient C was first evaluated at age 3, where she was referred to our Ophthalmic Genetics clinic due to a possible syndromic retinal degeneration, exotropia and difficulties with side and night vision. Outside records documented a failed newborn hearing screening bilaterally with an audiometric history documenting a progressive bilateral sensorineural hearing loss of a mild degree at 4 months of age to a moderate-to-severe hearing loss by 12 months of age. She received bilateral cochlear implants at 2 years of age. As a past medical history, she was born full term after a normal gestation, her height (56 cm), weight (3,591 g) and head circumference (34 cm) were on target and she presented with neonatal hypotonia that resolved shortly after. She also had palmar creases, facial asymmetry and dilated Aorta (Z-score >3). At age 2, she was diagnosed with mild developmental delay. Regarding her family history, her father, paternal grandmother and cousin had Marfan syndrome. Neuroimaging was performed and reportedly normal, but with many artifacts due to the metallic implants.

On our first evaluation, her BCVA was 20/200 binocularly (measured with Teller Acuity Cards). Her exam was also positive for exotropia, vertical nystagmus (OD more than OS) and her fundus showed granular macular changes, minimal vascular attenuation, light pigmentation, and peripheral patches of bony spicules. Autofluorescence imaging revealed a salt and pepper (hypo-hyperautofluorescence) on the midperiphery (Figure 1f). Her fingernails had mild bowing and a few leukonychia spots. At age 4, we could quantitatively evaluate her macular changes with OCT, being her CMT OD 406 μm and 466 μm OS, with cystic spaces on both eyes (Figure 1e). She passed the Ishihara color testing with 14 out of 16 plates read in each eye. Her axial length, keratometry and her IOP were within normal values. At age 5 years, an ERG was mostly extinguished OU. Her visual fields were mildly constricted; however, this was related with poor cooperation on the test due to young age. At this visit, she also had a developmental neuropsychological evaluation and was found to have extremely low to low average cognitive abilities (results from the cognitive test Wechsler Preschool and Primary Scale of Intelligence, Fourth Edition [WPPSI-IV]), with a relative strength in regards to her verbal comprehension skills and a significant weakness in regards to her visual spatial skills. Results of the Vineland Adaptive Behavior Scales, Second Edition indicated that her adaptive skills were largely in the moderately low range for her age but consistent with her cognitive profile (as measured by the WPPSI-IV). She demonstrated age appropriate adaptive behaviors in the socialization domain and was also found to be below average range for her age in both receptive (81 score in Peabody Picture Vocabulary Test, Fourth Edition [PPVT-4]) and expressive language skills (81 score in Expressive Vocabulary Test, Second Edition [EVT-2]). In the motor skills domain, her fine motor skills were rated to be age appropriate but her gross motor skills were moderately low. An electromyogram was also done in this consult and was within normal limits, with no electrophysiological evidence of a peripheral neuropathy.

Over the follow-up visits her nystagmus disappeared and the visual acuity oscillated around 20/200 OD and 20/100 OS. Her macular thickness remained being over 400 μm OU and her color vision did not decrease. Treatment with dorzolamide eye drops and oral acetazolamide was attempted but the macular changes were refractory to both drugs.

Given her complex phenotype, she was referred to the NIH Undiagnosed Diseases Clinic for further systemic workup. Over the 5 years of follow-up, she was diagnosed with Marfan

syndrome (molecular diagnosis prompted by family history). Usher syndrome and congenital disorders of glycosylation (CDG) were ruled out and at age 6 she was diagnosed with a peroxisomal disorder (molecular and biochemical diagnosis). She had a mixed dentition with primary teeth present and permanent teeth erupting. She had enamel loss on occlusal surfaces of her primary and permanent molars and her erupting mandibular incisors (Grade 4, Figure 2c). In addition to the enamel loss, Patient C also exhibited an unusual malocclusion where her mandibular teeth were in front of the maxillary teeth leading to crossbite and class III skeletal malocclusion. Her eruption pattern was slightly delayed for permanent dentition. Her panoramic X-ray showed multiple tooth buds for erupting permanent teeth and several retained primary teeth (asterisk, Figure 3c). CBCT images showed anterior teeth with even enamel thickness; however, the erupting central incisor had chipped upon eruption indicating weak enamel and dentin (Figure 3f). The erupting molars had irregular and hypo-mineralized enamel (red arrow heads, Figure 3f).

3.2 | Amelogenesis imperfecta

Regarding these patients' dental evaluation, mandibular first molars were also analyzed for volume comparison. Enamel volume was drastically reduced in all three patients than the normal levels (Figure 3g) (Kono, Suwa, & Tanijiri, 2002). Patient A had 65.08 cu.mm enamel volume on the mandibular first molar, with 18% of molar tooth surface covered by enamel. Patient B had 52.17 cu.mm of enamel volume that covered 15% of tooth surface whereas Patient C had 44.78 cu.mm of enamel covering 14% of the tooth. Dentin volume was measured only in the crown portion of the tooth and did not show any significant changes. Enamel varies in thickness over the surface of the tooth, often thickest at the cusp, up to 2.5 mm (Nanci, 2017). The average enamel thickness in the mandibular first molar in Patients A, B, and C were 1.82, 0.95, and 1.07 mm, respectively (Figure 3h). This data shows that Patient C was most severely affected followed by Patient B for having enamel loss and Patient A was least affected. The enamel loss pattern indicated reduced formation of enamel indicating amelogenesis imperfecta in all three patients.

3.3 | Biochemical

Patients A and B had a peroxisomal (C22, C24, C26, C24/C22, C:26/C:22, pristanic acid, phytanic acid, pristanic/phytanic) and hepatic panel, both within normal limits in the two patients. Patient C had elevated concentration of phytanic acid (3.85 μg/ml—normal <3.00 μg/ml), pristanic acid (1.68 μg/ml—normal <0.3 μg/ml), C24/C22 (1.205—normal up to 0.94), C26/C22 (0.055—normal up to 0.014), and C:26 (0.037%—normal 0.007%). C22:0 was mildly decreased (0.664%—normal 1.15%).

3.4 | Genetics

Patient A was found to have the variants c.1663T>C, p.(Ser555Pro) (variant of unknown significance—VUS, inherited paternally) and c.2097dup, p.(Ile700Tyrfs*42) (damaging, inherited maternally) in *PEX1* (NM_000466.2). Patient B had two compound heterozygous variants in trans in *PEX6* (NM_000287.3): c.1314_1321del, p.(Glu439Glyfs*3) (damaging), and c.133_147dup, p.(Glu45_Gly49dup) (VUS). Patient C had a homozygous c.2528G>A p.(Gly843Asp) pathogenic variant in *PEX1* and also carried a heterozygous c.7754T>C p.(Ile2585Thr) pathogenic variant in *FBN1* (inherited paternally).

4 | DISCUSSION

Classically, ZSDs were classified into SZ, NALD, and IRD (Zellweger, Maertens, Superneau, & Wertelecki, 1988). However, as other conditions were added to the group but did not fit the existing categories, new classifications regarding age of onset, and severity were proposed: neonatal-infantile, childhood, and adolescent-adult; severe, intermediate and mild (N. E. Braverman et al., 2016; Klouwer et al., 2016; Wanders, Klouwer, Ferdinandusse, Waterham, & Poll-Thé, 2017). ZS represents the most severe and earliest form of the disease that can be diagnosed in patients with fetal echogenic bowel, hypotonia, and craniofacial dysmorphism (Aydemir et al., 2014). These patients generally die before 1 year of age (S. J. Steinberg et al., 2017). NALD typically presents with failure to thrive during their first days of life, severe psychomotor retardation, development regression, and progressive hearing and vision loss (Farrell, 2012) and it is classified as intermediate severity. IRD has its onset during the first months of life presenting with developmental delay, ataxia, sensorineural hearing loss, bleeding episodes, and subtle dysmorphic facial features (Pakzad-Vaezi & Maberley, 2014). These patients' life expectancy is over 10 years of age and are grouped under the mild category, as well as HS and other patients presenting only with relatively isolated symptoms (Ebberink et al., 2010; Régal et al., 2010; Sevin, Ferdinandusse, Waterham, Wanders, & Aubourg, 2011).

It is important to differentiate HS from other ZSDs within the adult onset and mild subgroup. There are two main differences with IRD: HS lacks neurological manifestations and biochemical alterations (Suzuki et al., 2001). The remaining adolescent-adult onset disorders involve neurological manifestations such as ataxia and progressive spastic paraparesis (Ebberink et al., 2010; Régal et al., 2010; Sevin et al., 2011; Suzuki et al., 2001). To date, HS is the only ZSD with normal neurologic development, and for this reason the main differential diagnosis is not another peroxisomal disorder, but rather a ciliopathy, Usher syndrome (Raas-Rothschild et al., 2002). Given that the prevalence of Usher syndrome (around 1 in 6000) is more than 8 times the prevalence of all ZSDs, it is understandable that one may first consider a diagnosis of Usher syndrome in an infant with apparently isolated hearing and vision loss (Nagel-Wolfrum, Baasov, & Wolfrum, 2014). A detailed evaluation looking for amelogenesis imperfecta and nail abnormalities will help guide clinicians toward an early diagnosis of HS.

Another differential diagnosis to be taken into account is a Congenital disorder of glycosylation (CDG). This clinically heterogeneous group of diseases can present with retinal degeneration, sensorineural hearing loss, enamel defects and developmental delay, among many other manifestations (Chang, He, & Lam, 2018; Francisco et al., 2019; Morava et al., 2009; Rymen & Jaeken, 2014). Therefore, ruling out these conditions should be approached by analyzing the isoelectric focusing of serum transferrin and genetic testing (Francisco et al., 2019).

Our three cases demonstrate the usual diagnostic path that patients with mild peroxisomal diseases go though. The earliest complaint is hearing loss, which is often diagnosed in the first decade of life if not identified at birth secondary to failure of a newborn hearing screening. This is followed by amelogenesis imperfecta, which can be attributed to

nutritional factors, celiac disease or even idiopathic causes (Kanchan, Machado, Rao, Krishan, & Garg, 2015). The visual complaints depend on the severity of the macular changes. In the case of patients A and B, this was noticed in the second decade of life. These two patients have the classic characteristics of HS. Patient C presented with congenital progressive severe bilateral sensorineural hearing loss, developmental delay, abnormal peroxisomal panel and advanced retinal degeneration, at the youngest age of our cohort. The early macular changes occurred while she was in the critical period for developing amblyopia, therefore the lack of clear visual stimuli probably led to sensory strabismus, prompting an ophthalmic evaluation at a younger age.

Patient C's overall phenotype was more severe than the other two patients and she met the diagnostic criteria of IRD. The coexisting diagnosis of Marfan syndrome was unlikely to have contributed to this severity given the nonoverlapping nature of the associated phenotypes. Nevertheless, within IRD, the phenotype is very wide including patients with ataxia, hepatomegaly, intracranial bleeding and failure to thrive (Acharya, Ritwik, Velasquez, & Fenton, 2012). Furthermore, biochemical parameters in IRD also vary from moderately above normal limits to 10 times over the usual values (Matsui, Funahashi, Honda, & Shimozawa, 2013; Poll-The et al., 1987). By including patient C in our cohort, we intended to present a mild-moderate case to show how IRD, HS and peroxisomal disorders overlap and they are indeed a continuum. Therefore, we believe that categorizing these patients into mild, moderate and severe phenotypes gives us a better understanding of their global health.

4.1 | Pathophysiology and genetics

PEX1, PEX6, and PEX26 proteins interact in order to recycle PEX5, the cytosolic receptor for peroxisomal matrix proteins (peroxisomal targeting signals [PTS] 1 enzymes) (Tamura, Yasutake, Matsumoto, & Fujiki, 2006; Thoms & Erdmann, 2006; Yik, Steinberg, Moser, Moser, & Hacia, 2009). PEX1 and PEX6 are within the ATPases Associated with diverse cellular Activities (AAA) family of proteins and PEX26 is a peroxisomal membrane protein that maintains PEX1-PEX6 complex lodged to the membrane (Yik et al., 2009). Variants in either of the three genes encoding the mentioned proteins lead to a decreased activity of the PEX5-PTS1 complex (Okumoto, Miyata, & Fujiki, 2018). This not only causes a decreased catalytic activity toward VLCFA and other large molecules, but also a diminished synthesis of docosahexaenoic acid (DHA) (Ferdinandusse et al., 2001; Wanders & Waterham, 2004). DHA (C22:6n-3) is a polyunsaturated fatty acid of fundamental importance in cell membranes, which represents up to 50% of total FA in the phospholipids in nerve endings and photoreceptors. Its high concentration in the cerebral cortex and retina suggests a role in neural and visual function, and therefore the above described phenotype (Martinez, 1992; Martinez et al., 2010). The decreased activity of the PEX5-PTS1 complex leads to an inability to synthesize bile acids as well (Ferdinandusse et al., 2001). This causes an accumulation of the intermediates, di and trihydroxy-cholestanoic acid (DHCA and THCA), which are toxic to hepatocytes, explaining why hepatomegaly and hepatitis may be present in these patients (Heubi, Setchell, & Bove, 2018; Poll-The et al., 1987). They can also have hyperoxaluria and kidney stones, adrenal insufficiency and altered bone density (N. E. Braverman et al., 2016; van Woerden et al., 2006).

There are a total of 26 probands in the literature, 11 of which had a variant in *PEX1* (42%), 11 in *PEX6* (42%), 2 in *PEX26* (8%), and 2 had negative genetic testing (8%) (Gao et al., 2019; Mechaussier et al., 2019). Nineteen were missense variants (59%, 5 in *PEX1*, 11 in PEX6 and 3 in *PEX26*), nine were copy number variants or insertion/deletion (29%, 5 in *PEX1* and 4 in *PEX6*), two were splicing (6%, 1 in *PEX1* and 1 in *PEX6*) and two were nonsense (6%, 1 in *PEX1* and 1 in *PEX6*). One patient was homozygous in PEX1 and one in *PEX6*, while the rest were compound heterozygous. We added one novel variant in *PEX6* associated with HS: c.133_147dup, p.Glu45_Gly49dup. The variants associated with HS throughout the literature are illustrated in Figure 5.

One of the insertions in *PEX1* (c.2097dupT) was also reported in a patient with IRD, in trans with the missense c.2528G>A (Ghosh et al., 2017). The patient had developmental delay, facial dysmorphism and biochemical abnormalities. Also, the missense c.2528G>A was found in trans with c.760dupT in a patient with ZS (Cardoso, Amaral, Lemos, & Garcia, 2016). Regarding *PEX6*, c.1802G>A was described in a patient with development regression, biochemical abnormalities and brain leukodystrophy. This variant was in trans with c.2356C>T (Tran, Hewson, Steinberg, & Mercimek-Mahmutoglu, 2014). The remaining *PEX1* and *PEX6* variants related with HS to date were only seen in these patients or in cases of PBDs without clinical details. We did not find a genotype–phenotype correlation regarding particular alleles or regions of the proteins and HS. Gao et al. proposed a genotype–phenotype correlation in which the patients that had ocular involvement (retinal degeneration or macular cysts) had at least one variant affecting the AAA domain in *PEX1* or *PEX6* (Gao et al., 2019). We did not find this correlation in the three patients published by Mechaussier et al. or here, where the six patients had retinal degeneration and only two had a variant in the AAA domain (Mechaussier et al., 2019).

4.2 | Management

Several supportive therapeutic options have been evaluated for patients with PBDs. There are no clear recommendations regarding their diet (N. E. Braverman et al., 2016). Paker et al. evaluated DHA supplementation in patients with ZS, NALD and IRD and did not see any improvement of visual function or growth (Paker et al., 2010). Despite the limited number of patients in the literature treated with cholic acid supplementation (“Cholbam”), the United States Food and Drug Administration has approved its use to treat patients with peroxisomal disorders, including PBDs (FDA [Press Release], 2015; Setchell et al., 1992). This would decrease the accumulation of toxic bile acid precursors such as DHCA and THCA. Supplements of the fat-soluble vitamins such as A, D, E, and K are recommended (N. E. Braverman et al., 2016).

It is unclear however if these recommendations apply for milder PBDs such as HS. Since these patients are indeed affected by a peroxisomal disorder, an evaluation of associated features is certainly recommended. Early detection of adrenal insufficiency, low levels of fat-soluble vitamins, vitamin K dependent coagulopathy, liver and renal toxicity, and decreased bone density should be addressed. Developmental delay and visual impairment should be screened, and early intervention provided to the patient. Early diagnosis of amelogenesis imperfecta followed by restorations of affected tooth surfaces can help prolong the life of

teeth in these patients. Routine audiologic management and monitoring should accompany the diagnosis, particularly for those patients for whom congenital hearing loss is identified through newborn hearing screening. Because prepubescent bilateral hearing loss is often the first presenting symptom, it is critical to establish appropriate hearing healthcare through proper audiologic and otolaryngologic management. Further evaluation will depend on the case and the screening results.

In summary, mild peroxisomal disorders should be suspected in every child with hearing loss and visual disturbance. A thorough systemic evaluation focused on dental and nail anomalies, followed by a peroxisomal panel and genetic testing are critical steps for patients in which HS is suspected. Appropriate diagnosis can lead to better management of the associated complications and timely genetic counseling.

Acknowledgments

Funding information

Intramural Research Funds from the National Eye Institute; Intramural Research Funds from the National Institute of Dental and Craniofacial Research; Intramural Research Funds from the National Institute on Deafness and Other Communication Disorders; Intramural Research Funds from the NIH Undiagnosed Diseases Program

REFERENCES

Acharya BS, Ritwik P, Velasquez GM, & Fenton SJ (2012). Medical-dental findings and management of a child with infantile Refsum disease: A case report. Special Care in Dentistry, 32(3), 112–117. 10.1111/j.1754-4505.2012.00248.x [PubMed: 22591434]

Aydemir O, Kavurt S, Esin S, Kandemir O, Bas AY, & Demirel N (2014). Fetal echogenic bowel in association with Zellweger syndrome. Journal of Obstetrics and Gynaecology Research, 40(6), 1799–1802. 10.1111/jog.12379

Bodman MA (2004). Nail dystrophies. Clinics in Podiatric Medicine and Surgery, 21(4), 663–687. 10.1016/j.cpm.2004.05.005 [PubMed: 15450905]

Braverman N, Argyriou C, & Moser A (2014). Human disorders of peroxisome biogenesis: Zellweger spectrum and rhizomelic chondrodysplasia punctata. In Molecular machines involved in peroxisome biogenesis and maintenance (pp. 63–90). Vienna, Austria: Springer.

Braverman NE, Raymond GV, Rizzo WB, Moser AB, Wilkinson ME, Stone EM, … Bose M (2016). Peroxisome biogenesis disorders in the Zellweger spectrum: An overview of current diagnosis, clinical manifestations, and treatment guidelines. Molecular Genetics and Metabolism, 117(3), 313–321. 10.1016/j.ymgme.2015.12.009 [PubMed: 26750748]

Brown FR 3rd, McAdams AJ, Cummins JW, Konkol R, Singh I, Moser AB, & Moser HW (1982). Cerebro-hepato-renal (Zellweger) syndrome and neonatal adrenoleukodystrophy: Similarities in phenotype and accumulation of very long chain fatty acids. Johns Hopkins Medical Journal, 151(6), 344–351.

Cardoso P, Amaral ME, Lemos S, & Garcia P (2016). Zellweger syndrome with severe malnutrition, immunocompromised state and opportunistic infections. BMJ Case Reports, 2016, bcr2015214283. 10.1136/bcr-2015-214283

Chang IJ, He M, & Lam CT (2018). Congenital disorders of glycosylation. Annals of Translational Medicine, 6(24), 477–477. 10.21037/atm.2018.10.45 [PubMed: 30740408]

Delille HK, Bonekamp NA, & Schrader M (2006). Peroxisomes and disease—An overview. International Journal of Biomedical Science: IJBS, 2(4), 308–314 Retrieved from https://pubmed.ncbi.nlm.nih.gov/23674998; https://www.ncbi.nlm.nih.gov/pmc/articles/PMC3614646/ [PubMed: 23674998]

Ebberink MS, Csanyi B, Chong WK, Denis S, Sharp P, Mooijer PAW, … Ferdinandusse S (2010). Identification of an unusual variant peroxisome biogenesis disorder caused by mutations in the

PEX16 gene. Journal of Medical Genetics, 47(9), 608–615. 10.1136/jmg.2009.074302 [PubMed: 20647552]

Farrell DF (2012). Neonatal adrenoleukodystrophy: A clinical, pathologic, and biochemical study. Pediatric Neurology, 47(5), 330–336. 10.1016/j.pediatrneurol.2012.07.006 [PubMed: 23044013]

Ferdinandusse S, Denis S, Mooijer PAW, Zhang Z, Reddy JK, Spector AA, & Wanders RJA (2001). Identification of the peroxisomal β-oxidation enzymes involved in the biosynthesis of docosahexaenoic acid. Journal of Lipid Research, 42(12), 1987–1995 Retrieved from http://www.jlr.org/content/42/12/1987.abstract [PubMed: 11734571]

Francisco R, Marques-da-Silva D, Brasil S, Pascoal C, dos Reis Ferreira V, Morava E, & Jaeken J (2019). The challenge of CDG diagnosis. Molecular Genetics and Metabolism, 126(1), 1–5. 10.1016/j.ymgme.2018.11.003 [PubMed: 30454869]

Gao F-J, Hu F-Y, Xu P, Qi Y-H, Li J-K, Zhang Y, … Wu J-H (2019). Expanding the clinical and genetic spectrum of Heimler syndrome. Orphanet Journal of Rare Diseases, 14(1), 290. 10.1186/s13023-019-1243-x [PubMed: 31831025]

Ghosh A, Schlecht H, Heptinstall LE, Bassett JK, Cartwright E, Bhaskar SS, … Banka S (2017). Diagnosing childhood-onset inborn errors of metabolism by next-generation sequencing. Archives of Disease in Childhood, 102(11), 1019–1029. 10.1136/archdischild-2017-312738 [PubMed: 28468868]

Goldfischer S, Moore CL, Johnson AB, Spiro AJ, Valsamis MP, Wisniewski HK, … Gartner LM (1973). Peroxisomal and mitochondrial defects in the cerebro-hepato-renal syndrome. Science, 182(4107), 62–64. 10.1126/science.182.4107.62 [PubMed: 4730055]

Heimler A, Fox JE, Hershey JE, & Crespi P (1991). Sensorineural hearing loss, enamel hypoplasia, and nail abnormalities in sibs. American Journal of Medical Genetics, 39(2), 192–195. 10.1002/ajmg.1320390214 [PubMed: 2063923]

Heubi JE, Setchell KDR, & Bove KE (2018). Inborn errors of bile acid metabolism. Clinics in Liver Disease, 22(4), 671–687. 10.1016/j.cld.2018.06.006 [PubMed: 30266156]

Jani P, Nguyen QC, Almpani K, Keyvanfar C, Mishra R, Liberton D, … Lee JS (2020). Severity of oro-dental anomalies in Loeys– Dietz syndrome segregates by gene mutation. Journal of Medical Genetics. 10.1136/jmedgenet-2019-106678

Kanchan T, Machado M, Rao A, Krishan K, & Garg A (2015). Enamel hypoplasia and its role in identification of individuals: A review of literature. Indian Journal of Dentistry, 6(2), 99–102. 10.4103/0975-962x.155887 [PubMed: 26097340]

Kelley RI, & Moser HW (1984). Hyperpipecolic acidemia in neonatal adrenoleukodystrophy. American Journal of Medical Genetics, 19(4), 791–795. 10.1002/ajmg.1320190420 [PubMed: 6517102]

Klouwer FCC, Berendse K, Ferdinandusse S, Wanders RJA, Engelen M, & Poll-The BT (2015). Zellweger spectrum disorders: Clinical overview and management approach. Orphanet Journal of Rare Diseases, 10(1), 151. 10.1186/s13023-015-0368-9 [PubMed: 26627182]

Klouwer FCC, Ferdinandusse S, van Lenthe H, Kulik W, Wanders RJA, Poll-The BT, … Vaz FM (2017). Evaluation of C26:0-lysophosphatidylcholine and C26:0-carnitine as diagnostic markers for Zellweger spectrum disorders. Journal of Inherited Metabolic Disease, 40(6), 875–881. 10.1007/s10545-017-0064-0 [PubMed: 28677031]

Klouwer FCC, Huffnagel IC, Ferdinandusse S, Waterham HR, Wanders RJA, Engelen M, & Poll-The BT (2016). Clinical and biochemical pitfalls in the diagnosis of peroxisomal disorders. Neuropediatrics, 47(4), 205–220. 10.1055/s-0036-1582140 [PubMed: 27089543]

Kono RT, Suwa G, & Tanijiri T (2002). A three-dimensional analysis of enamel distribution patterns in human permanent first molars. Archives of Oral Biology, 47(12), 867–875. 10.1016/s0003-9969(02)00151-6 [PubMed: 12450518]

Lee PR, & Raymond GV (2013). Child neurology: Zellweger syndrome. Neurology, 80(20), e207–e210. 10.1212/wnl.0b013e3182929f8e [PubMed: 23671347]

Lima LH, Barbazetto IA, Chen R, Yannuzzi LA, Tsang SH, & Spaide RF (2011). Macular dystrophy in Heimler syndrome. Ophthalmic Genetics, 32(2), 97–100. 10.3109/13816810.2010.551797 [PubMed: 21366429]

Lipiński P, Stawiński P, Rydzanicz M, Wypchło M, Płoski R, Stradomska TJ, … Tylki-Szymańska A (2020). Mild Zellweger syndrome due to functionally confirmed novel PEX1 variants. Journal of Applied Genetics, 61(1), 87–91. 10.1007/s13353-019-00523-w [PubMed: 31628608]

Marmor MF, Fulton AB, Holder GE, Miyake Y, Brigell M, & Bach M (2008). ISCEV standard for full-field clinical electroretinography (2008 update). Documenta Ophthalmologica, 118(1), 69–77. 10.1007/s10633-008-9155-4 [PubMed: 19030905]

Martinez M (1992). Abnormal profiles of polyunsaturated fatty acids in the brain, liver, kidney and retina of patients with peroxisomal disorders. Brain Research, 583(1–2), 171–182. 10.1016/s0006-8993(10)80021-6 [PubMed: 1504825]

Martinez M, Ichaso N, Setien F, Durany N, Qiu X, & Roesler W (2010). The Δ4-desaturation pathway for DHA biosynthesis is operative in the human species: Differences between normal controls and children with the Zellweger syndrome. Lipids in Health and Disease, 9(1), 98. 10.1186/1476-511x-9-98 [PubMed: 20828389]

Matsui S, Funahashi M, Honda A, & Shimozawa N (2013). Newly identified milder phenotype of peroxisome biogenesis disorder caused by mutated PEX3 gene. Brain and Development, 35(9), 842–848. 10.1016/j.braindev.2012.10.017 [PubMed: 23245813]

McCulloch DL, Marmor MF, Brigell MG, Hamilton R, Holder GE, Tzekov R, & Bach M (2014). ISCEV standard for full-field clinical electroretinography (2015 update). Documenta Ophthalmologica, 130(1), 1–12. 10.1007/s10633-014-9473-7 [PubMed: 25502644]

Mechaussier S, Marlin S, Kaplan J, Rozet J-M, & Perrault I (2019). Genetic deciphering of early-onset and severe retinal dystrophy associated with sensorineural hearing loss. In Retinal degenerative diseases (pp. 233–238). Cham, Switzerland: Springer International Publishing.

Morava E, Wosik HN, Sykut-Cegielska J, Adamowicz M, Guillard M, Wevers RA, … Cruysberg JRM (2009). Ophthalmological abnormalities in children with congenital disorders of glycosylation type I. British Journal of Ophthalmology, 93(3), 350–354. 10.1136/bjo.2008.145359

Nagel-Wolfrum K, Baasov T, & Wolfrum U (2014). Therapy strategies for usher syndrome type 1C in the retina. In Retinal degenerative diseases (pp. 741–747). New York, NY: Springer.

Nanci A (2017). Ten Cate's oral histology-E-book: Development, structure, and function, St. Louis, Missouri: Elsevier Health Sciences.

Neuhaus C, Eisenberger T, Decker C, Nagl S, Blank C, Pfister M, … Bolz HJ (2017). Next-generation sequencing reveals the mutational landscape of clinically diagnosed Usher syndrome: Copy number variations, phenocopies, a predominant target for translational read-through, and PEX26mutated in Heimler syndrome. Molecular Genetics & Genomic Medicine, 5(5), 531–552. 10.1002/mgg3.312 [PubMed: 28944237]

Okumoto K, Miyata N, & Fujiki Y (2018). Identification of peroxisomal protein complexes with PTS receptors, Pex5 and Pex7, in mammalian cells. In Proteomics of peroxisomes (pp. 287–298). Singapore: Springer.

Oliveira C, Harizman N, Girkin CA, Xie A, Tello C, Liebmann JM, & Ritch R (2007). Axial length and optic disc size in normal eyes. British Journal of Ophthalmology, 91(1), 37–39. 10.1136/bjo.2006.102061

Ong KR, Visram S, McKaig S, & Brueton LA (2006). Sensorineural deafness, enamel abnormalities and nail abnormalities: A case report of Heimler syndrome in identical twin girls. European Journal of Medical Genetics, 49(2), 187–193. 10.1016/j.ejmg.2005.07.003 [PubMed: 16530715]

Opitz JM (1969). The Zellweger syndrome (cerebro-hepato-renal syndrome). Birth Defects Original Article Series, 5, 144–158.

Paker AM, Sunness JS, Brereton NH, Speedie LJ, Albanna L, Dharmaraj S, … Raymond GV (2010). Docosahexaenoic acid therapy in peroxisomal diseases: Results of a double-blind, randomized trial. Neurology, 75(9), 826–830. 10.1212/wnl.0b013e3181f07061 [PubMed: 20805528]

Pakzad-Vaezi KL, & Maberley DAL (2014). Infantile Refsum disease in a young adult. Retinal Cases & Brief Reports, 8(1), 56–59. 10.1097/icb.0000000000000004 [PubMed: 25372210]

Peduto A, Baumgartner MR, Verhoeven NM, Rabier D, Spada M, Nassogne M-C, … Saudubray J-M (2004). Hyperpipecolic acidaemia: a diagnostic tool for peroxisomal disorders. Molecular Genetics and Metabolism, 82(3), 224–230. 10.1016/j.ymgme.2004.04.010 [PubMed: 15234336]

Poll-The BT, Saudubray JM, Ogier HAM, Odivre M, Scotto JM, Monnens L, … Tager JM (1987). Infantile Refsum disease: An inherited peroxisomal disorder. European Journal of Pediatrics, 146(5), 477–483. 10.1007/bf00441598 [PubMed: 2445576]

Poulos A, Sharp P, & Whiting M (1984). Infantile Refsum's disease (phytanic acid storage disease): A variant of Zellweger's syndrome? Clinical Genetics, 26(6), 579–586. 10.1111/j.1399-0004.1984.tb01107.x [PubMed: 6209040]

Raas-Rothschild A, Wanders RJA, Mooijer PAW, Gootjes J, Waterham HR, Gutman A, … Korman SH (2002). A PEX6-defective peroxisomal biogenesis disorder with severe phenotype in an infant, versus mild phenotype resembling usher syndrome in the affected parents. The American Journal of Human Genetics, 70(4), 1062–1068. 10.1086/339766 [PubMed: 11873320]

Ratbi I, Falkenberg KD, Sommen M, Al-Sheqaih N, Guaoua S, Vandeweyer G, Van Camp G (2015). Heimler syndrome is caused by hypomorphic mutations in the peroxisome-biogenesis genes PEX1 and PEX6. The American Journal of Human Genetics, 97(4), 535–545. 10.1016/j.ajhg.2015.08.011 [PubMed: 26387595]

Régal L, S M, Goemans N, Wanders RJA, De Meirleir L, Jaeken J, … Waterham HR (2010). Mutations in PEX10 are a cause of autosomal recessive ataxia. Annals of Neurology, 68(2), 259–263. 10.1002/ana.22035 [PubMed: 20695019]

Richards S, Aziz N, Bale S, Bick D, Das S, Gastier-Foster J, … Rehm HL (2015). Standards and guidelines for the interpretation of sequence variants: A joint consensus recommendation of the American College of Medical Genetics and Genomics and the Association for Molecular Pathology. Genetics in Medicine, 17(5), 405–423. 10.1038/gim.2015.30 [PubMed: 25741868]

Rosewich H (2005). Genetic and clinical aspects of Zellweger spectrum patients with PEX1 mutations. Journal of Medical Genetics, 42(9), e58. 10.1136/jmg.2005.033324 [PubMed: 16141001]

Rymen D, & Jaeken J (2014). Skin manifestations in CDG. Journal of Inherited Metabolic Disease, 37(5), 699–708. 10.1007/s10545-014-9678-7 [PubMed: 24554337]

Setchell KDR, Bragetti P, Zimmer-Nechemias L, Daugherty C, Pelli MA, Vaccaro R, … Clerici C (1992). Oral bile acid treatment and the patient with Zellweger syndrome. Hepatology, 15(2), 198–207. 10.1002/hep.1840150206 [PubMed: 1735522]

Sevin C, Ferdinandusse S, Waterham HR, Wanders RJ, & Aubourg P (2011). Autosomal recessive cerebellar ataxia caused by mutations in the PEX2 gene. Orphanet Journal of Rare Diseases, 6(8), 1–4. 10.1186/1750-1172-6-8 [PubMed: 21235735]

Smith CEL, Poulter JA, Levin AV, Capasso JE, Price S, Ben-Yosef T, … Inglehearn CF (2016). Spectrum of PEX1 and PEX6 variants in Heimler syndrome. European Journal of Human Genetics, 24(11), 1565–1571. 10.1038/ejhg.2016.62 [PubMed: 27302843]

Steinberg S, Chen L, Wei L, Moser A, Moser H, Cutting G, & Braverman N (2004). The PEX gene screen: Molecular diagnosis of peroxisome biogenesis disorders in the Zellweger syndrome spectrum. Molecular Genetics and Metabolism, 83(3), 252–263. 10.1016/j.ymgme.2004.08.008 [PubMed: 15542397]

Steinberg S, Jones R, Tiffany C, & Moser A (2008). Investigational methods for peroxisomal disorders. Current Protocols in Human Genetics, 58(1), 17.16.11–17.16.23. 10.1002/0471142905.hg1706s58

Steinberg SJ, Raymond GV, Braverman NE, & Moser AB (2017). Zellweger spectrum disorder. In GeneReviews® (Internet). Seattle, WA: University of Washington.

Suzuki Y, Shimozawa N, Imamura A, Fukuda S, Zhang Z, Orii T, & Kondo N (2001). Clinical, biochemical and genetic aspects and neuronal migration in peroxisome biogenesis disorders. Journal of Inherited Metabolic Disease, 24(2), 151–165. 10.1023/A:1010310816743 [PubMed: 11405337]

Tamura S, Yasutake S, Matsumoto N, & Fujiki Y (2006). Dynamic and functional assembly of the AAA peroxins, Pex1p and Pex6p, and their membrane receptor Pex26p. Journal of Biological Chemistry, 281(38), 27693–27704. 10.1074/jbc.m605159200

Tan AP, Gonçalves FG, Almehdar A, & Soares BP (2018). Clinical and neuroimaging spectrum of peroxisomal disorders. Topics in Magnetic Resonance Imaging, 27(4), 241–257. 10.1097/rmr.0000000000000172 [PubMed: 30086110]

Theda C, Woody RC, Naidu S, Moser AB, & Moser HW (1993). Increased very long chain fatty acids in patients on a ketogenic diet: A cause of diagnostic confusion. The Journal of Pediatrics, 122(5), 724–726. 10.1016/s0022-3476(06)80013-2 [PubMed: 8496750]

Thoms S, & Erdmann R (2006). Peroxisomal matrix protein receptor ubiquitination and recycling. Biochimica et Biophysica Acta (BBA)-Molecular Cell Research, 1763(12), 1620–1628. 10.1016/j.bbamcr.2006.08.046 [PubMed: 17028012]

Tran C, Hewson S, Steinberg SJ, & Mercimek-Mahmutoglu S (2014). Late-onset Zellweger spectrum disorder caused by PEX6 mutations mimicking X-linked adrenoleukodystrophy. Pediatric Neurology, 51(2), 262–265. 10.1016/j.pediatrneurol.2014.03.020 [PubMed: 25079577]

United States Food and Drug Administration. (2015). FDA approves Cholbam to treat rare bile acid synthesis disorders. Press release. Retrieved from http://www.fda.gov/NewsEvents/Newsroom/PressAnnouncements/ucm438572.htm

van Woerden CS, Groothoff JW, Wijburg FA, Duran M, Wanders RJA, Barth PG, & Poll-The BT (2006). High incidence of hyperoxaluria in generalized peroxisomal disorders. Molecular Genetics and Metabolism, 88(4), 346–350. 10.1016/j.ymgme.2006.03.004 [PubMed: 16621644]

Vasiljevic E, Ye Z, Pavelec DM, Darst BF, Engelman CD, & Baker MW (2019). Carrier frequency estimation of Zellweger spectrum disorder using ExAC database and bioinformatics tools. Genetics in Medicine, 21(9), 1969–1976. 10.1038/s41436-019-0468-3 [PubMed: 30846882]

Ventura MJ, Wheaton D, Xu M, Birch D, Bowne SJ, Sullivan LS, … Wangler MF (2016). Diagnosis of a mild peroxisomal phenotype with next-generation sequencing. Molecular Genetics and Metabolism Reports, 9, 75–78. 10.1016/j.ymgmr.2016.10.006 [PubMed: 27872819]

Walter C, Gootjes J, Mooijer PA, Portsteffen H, Klein C, Waterham HR, … Dodt G (2001). Disorders of peroxisome biogenesis due to mutations in PEX1: Phenotypes and PEX1 protein levels. The American Journal of Human Genetics, 69(1), 35–48. 10.1086/321265 [PubMed: 11389485]

Wanders RJA, Klouwer FCC, Ferdinandusse S, Waterham HR, & Poll-Thé BT (2017). Clinical and laboratory diagnosis of peroxisomal disorders. In Methods in molecular biology (pp. 329–342). New York, NY: Springer.

Wanders RJA, & Waterham HR (2004). Peroxisomal disorders. I: Biochemistry and genetics of peroxisome biogenesis disorders. Clinical Genetics, 67(2), 107–133. 10.1111/j.1399-0004.2004.00329.x

Wanders RJA, & Waterham HR (2006). Biochemistry of mammalian peroxisomes revisited. Annual Review of Biochemistry, 75(1), 295–332. 10.1146/annurev.biochem.74.082803.133329

Yik WY, Steinberg SJ, Moser AB, Moser HW, & Hacia JG (2009). Identification of novel mutations and sequence variation in the Zellweger syndrome spectrum of peroxisome biogenesis disorders. Human Mutation, 30(3), E467–E480. 10.1002/humu.20932 [PubMed: 19105186]

Zeharia A, Ebberink MS, Wanders RJA, Waterham HR, Gutman A, Nissenkorn A, & Korman SH (2007). A novel PEX12 mutation identified as the cause of a peroxisomal biogenesis disorder with mild clinical phenotype, mild biochemical abnormalities in fibroblasts and a mosaic catalase immunofluorescence pattern, even at 40°C. Journal of Human Genetics, 52(7), 599–606. 10.1007/s10038-007-0157-y [PubMed: 17534573]

Zellweger H, Maertens P, Superneau D, & Wertelecki W (1988). History of the cerebrohepatorenal syndrome of Zellweger and other peroxisomal disorders. Southern Medical Journal, 81(3), 357–364. 10.1097/00007611-198803000-00017 [PubMed: 2450404]

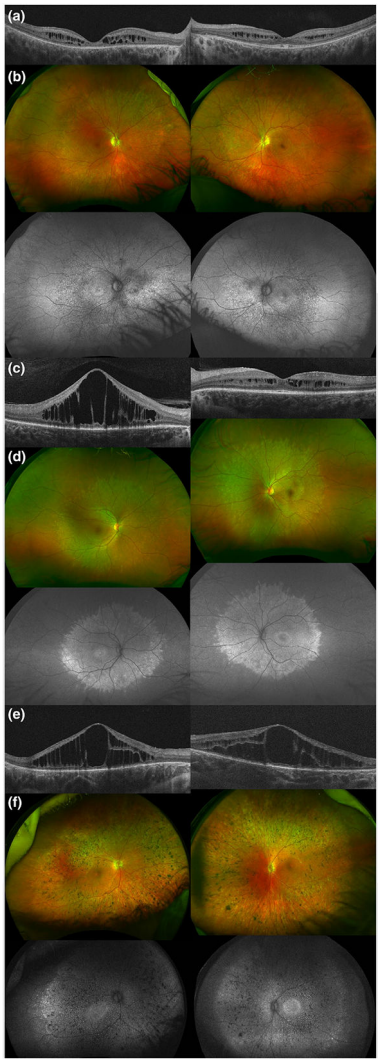

FIGURE 1.

Ophthalmologic characteristics of patients with mild peroxisomal biogenesis disorders. (a, c, and e) Macular optical coherence tomography images of Patients A, B, and C, respectively, showing cystic spaces and discontinuity of the outer retinal layers. (b and d) Color and autofluorescence ultrawide-field retinal images of patients with Heimler syndrome (Patients A and B). Their retinal dystrophy is characterized by few pigment redistribution, mild vessel attenuation, and a mostly mid-peripheral involvement with a hyper-hypoautofluorescence pattern. (f) Color and autofluorescence ultrawide-field retinal images of Patient C. In this case, we notice pigment clumping throughout the retina, moderate–severe vessel thinning, and a more extensive hyper-hypoautofluorescence (“salt and pepper”) pattern

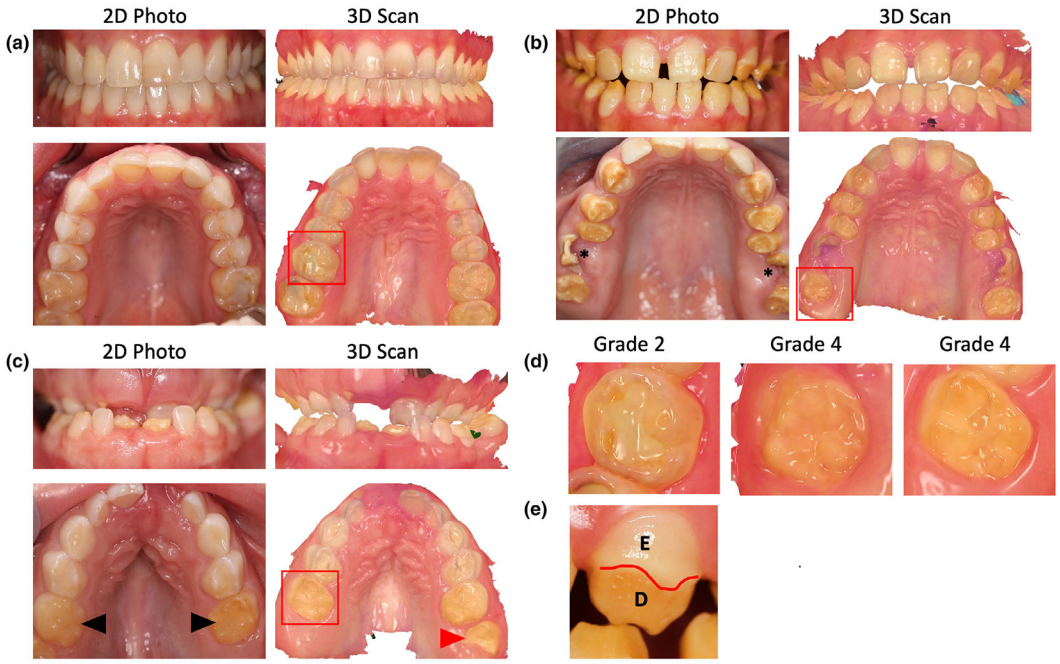

FIGURE 2.

(a) Front view of teeth in Patient A as seen in 2D photo and 3D intraoral scan in the top row. Bottom row shows the occlusal view of the upper (maxillary) teeth in the 2D and 3D views, respectively. The Grade 2 enamel loss was restricted to the molars in upper and lower arch of Patient A. (b) 2D photos and 3D scans of Patient B showing enamel loss affecting all teeth except the incisors. The upper first molars were severely broken (asterisk) and enamel was lost on all surfaces of affected teeth. (c) Patient C had most primary teeth that were unaffected except the second molars (black arrowhead). The erupting first molars (red arrowhead) and incisors had severe enamel loss indicating a Grade 4 enamel defect. (d) Magnified view of the molars marked by red box from Patients A, B, and C showing the severity of enamel loss. (e) Facial surface of canine tooth in Patient B showing partial enamel loss marked by red line. E, enamel, D, dentin

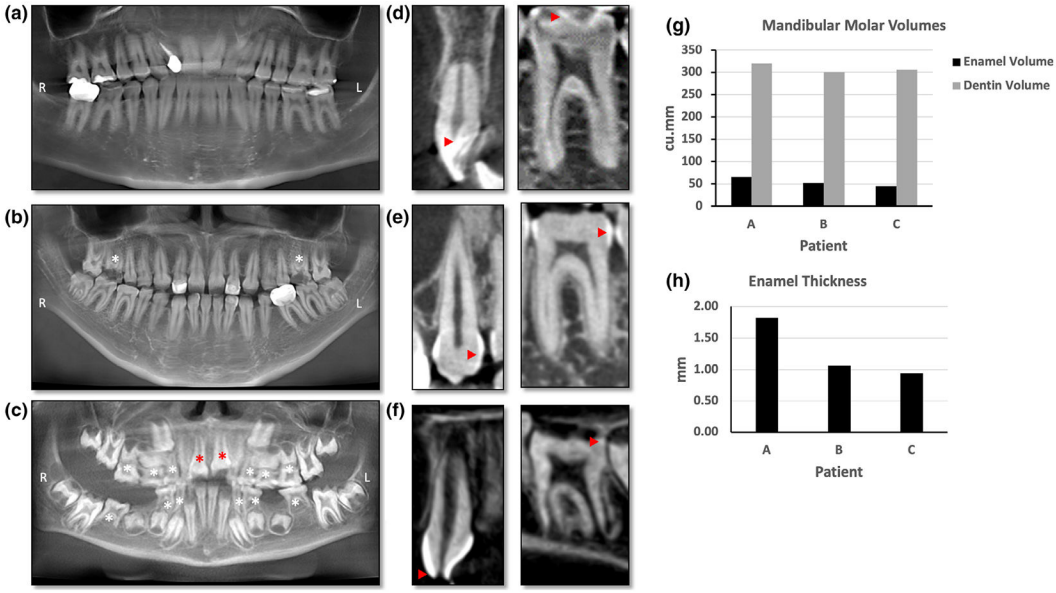

FIGURE 3.

(a–c) Panoramic X-ray reformatted from CBCT. (d–f) Sagittal slice through an anterior (left panel) and one posterior tooth (right panel) from the cone-beam computed tomography scans. (a) Panoramic X-ray of Patient A showing multiple restorations. Enamel is seen as the thin white line outlining the teeth. Several posterior teeth needed restoration due to loss of enamel. (b) Patient B had three restorations visible on the panoramic X-ray and both maxillary first molars have broken crowns (white asterisk) and pulp exposure due to severe enamel loss. (c) Panoramic X-ray of Patient C showing retained primary teeth (white asterisk) and multiple unerupted permanent teeth. The erupting central incisors (red asterisk) seem to have broken incisal edges indicating hypoplastic enamel. (d) Left panel shows 2D slice through anterior tooth in Patient A with normal enamel (red arrowhead). Right panel shows a 2D slice through the molar with thin enamel (red arrowhead). (e) Anterior tooth enamel is irregular and thin on the left panel in Patient B whereas the molar on right panel has no enamel on the occlusal surface and thin enamel on the proximal surface (red arrow heads). (f) Patient C has broken incisal edge with exposed pulp cavity (red arrowhead) of the anterior tooth in left panel. Right panel shows an erupting molar with irregular and patchy enamel seen as white to light gray dots red arrowhead). (g) Bar graph comparing the volumes of enamel and dentin in the three patients. Patients A, B, and C had 65.08, 52.17, and 44.78 cu.mm of enamel, respectively. (h) Bar graph comparing the thickness of enamel in all three patients. The enamel thickness was 1.82, 0.95, and 1.07 mm in Patients A, B, and C, respectively. R: Right, L: Left

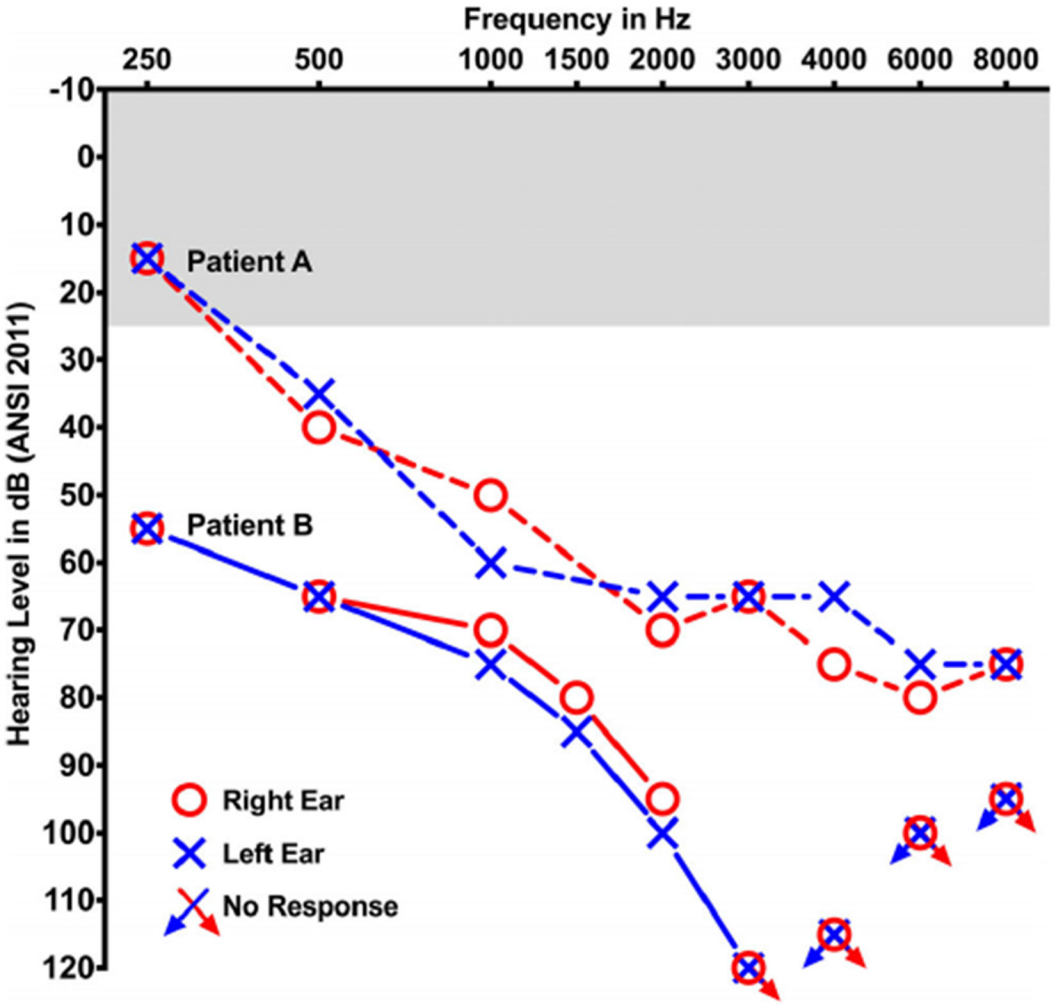

FIGURE 4.

Audiograms representing air conduction thresholds for the right (red) and left (blue) ears of Patient A (dashed lines) and Patient B (solid lines). Bone conduction thresholds (not shown) were equal to air conduction thresholds. Shaded gray denotes range of normal hearing sensitivity

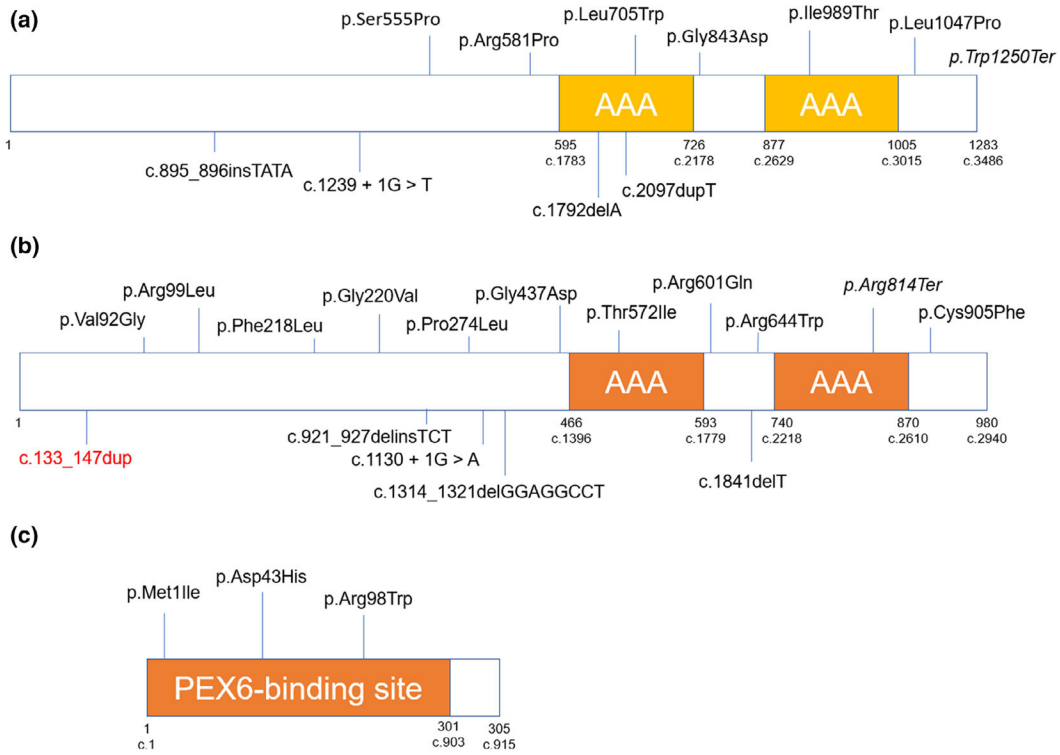

FIGURE 5.

Variants associated with Heimler syndrome to date. (a) PEX1 protein, (b) PEX6, and (c) PEX26. Missense and nonsense variants are shown above the diagram; splicing, insertions, deletions, and copy-number variations are underneath